Proceedings of the 8th IFAC International Conference on
Manoeuvring and Control of Marine Craft
September 16-18, 2009, Guarujá (SP), Brazil

DEVELOPMENT AND APPLICATION OF A SHIP MANOEUVRING DIGITAL SIMULATOR FOR RESTRICTED WATERS

Jessé Rebello de Souza Junior[*], Eduardo A. Tannuri [**], Anderson T. Oshiro[***], Helio M. Morishita[****]

[*] *Dept. of Naval Architecture and Ocean Engineering, University of São Paulo, (e-mail: jsouza@usp.br)*
[**] *Dept. of Mechatronics Engineering, University of São Paulo, (e-mail: eduat@usp.br)*
[***] *Dept. of Naval Architecture and Ocean Engineering, University of São Paulo, (e-mail: anderson.oshiro@poli.usp.br)*
[****] *Dept. of Naval Architecture and Ocean Engineering, University of São Paulo, (e-mail: hmmorish@usp.br)*

Abstract: This paper reports on two case studies making use of a digital simulator to investigate the manoeuvring motions of ships in canals with shallow and restricted waters. The first case study corresponds to a manoeuvring analysis conducted for the Port of Rio Grande (RS - Brazil), whose aim was to assess the potential impact upon manoeuvres of the presence of a large offshore platform (the Petrobras P-53) which is to remain docked for several months at the Port to complete its construction. The second study made use of the simulator to evaluate the manoeuvring conditions along the approach route and manoeuvring basin of the Port of Ponta do Félix (PR – Brazil). The simulator includes a complete mathematical model of the ship dynamics in the horizontal plane when subjected to wind and current forces. It also comprises detailed models for the action of thrusters and propellers, both fixed and azimuth, employed to control manoeuvres and dynamically position ships, as well as rudders and tugboats. The models used by the simulator allow for the effects of shallow and restricted waters, including the increase in resistance and lateral forces, increase in additional mass and the appearance of lateral and vertical suction (squatting). The simulator is implemented via an interactive interface through which the user is able to apply control actions (rudder angle, main engine, thrusters and tugboats) in real time during manoeuvres, thereby reproducing to some extent the action of a pilot.

Keywords: Manoeuvring

1. INTRODUCTION

The pursuit of increased competitiveness throughout the chain of river and maritime transportation services has placed growing strains over the safety restrictions imposed upon the navigation along access waterways and on ship manoeuvres. Factors that are crucial for safety, such as the dimensions of channels and manoeuvring basins relative to ship size have been under close scrutiny. The Department of Naval Architecture and Ocean Engineering and the Department of Mechatronics Engineering of the University of São Paulo have been developing a computer simulation tool to evaluate the motions of vessels in situations of restricted depth and width. The simulator can be useful in dealing with complex problems that arise at the interface between the operability of the system and the safety of operations: dimensioning of areas and depths of passage, simulation of the (positive or negative) impact on safety of changes in navigation conditions, and analysis of the possibility of reduction of restriction to manoeuvres, amongst others.

Recently, the simulator was employed in two real-world studies. It was used to investigate the impact on the safety of manoeuvres at the Port of Rio Grande (Brazil) of the presence of a large oil platform which was docked at the harbour for completion of its construction. For the Terminal of Ponta do Félix (Brazil), the simulator was used to assess the manoeuvring conditions of a new, larger type of vessel.

All the main physical phenomena of interest to the realistic reproduction of ship manoeuvring motions are represented in the mathematical models that constitute the core of the simulator. From the step-by-step calculation of forces and moments acting upon the ship the simulator performs a numerical time integration to generate ship trajectories. These are animated in a bird's eye, two-dimensional graphical representation of the navigation area, allowing the operator (who plays the role of the ship's pilot) to conduct the manoeuvres by commanding power, steering, and tugboat parameters.

2. MATHEMATICAL MODELLING

This section will present the mathematical models included in the simulator and will provide the basic data for modelling of ships covered in the case studies that will be discussed throughout this work.

2.1 BASIC DATA OF THE VESSELS

The ship considered in the case study of the Port of Rio Grande was the Grimaldi Ro-Ro, Class Grande Francia. Henceforth this ship is referred to as vessel A. For the study of the Port of Antonina, the ship considered is the Star Class

H type open hatch (referred to as vessel B). Photos of the ships are shown in Figures 1 and 2.

Figure 1 - H Star Ship (Vessel B)

Figure 2 - Ro-Ro vessel (Vessel A)

The main data of the vessels are given in Table 1.

Table 1 Vessel's Data

Feature	Vessel A	Vessel B
Length (LOA)	214,0m	213,4m
Beam (B)	32,25m	31,00m
Draft (T)	8,23m	8,10m
Mass (m)	48561 ton	40672 ton
Mom. Inertia (Iz)	$1{,}24.10^8$ ton.m^2	$1{,}05.10^8$ ton.m^2
Wetted Area (S)	7222 m^2	7025 m^2
CG's Position	0m	0m
Block Coeff. (Cb)	0,83	0,80

2.2 WIND FORCES

The forces in the longitudinal direction (surge) and lateral (sway) and the yaw moment (yaw) due to the effect of wind on the emerged part of the vessel are modelled by the wind coefficients. Assuming that there is no spatial variation in speed and direction of wind incident on the vessel, the following relationships are assumed:

$$F_{1V} = \frac{1}{2}\rho_a C_{Vx}(\beta_V) A_F V^2 \quad F_{2V} = \frac{1}{2}\rho_a C_{Vy}(\beta_V) A_L V^2 \quad F_{6V} = \frac{1}{2}\rho_a C_{Vn}(\beta_V) L A_L V^2 \qquad (1)$$

where ρ is the density of air, F_{1V} and F_{2V} are forces in the longitudinal and transverse directions respectively, F_{6V} is the moment of yaw, C_{VX}, C_{Vy} and C_{VN} are dimensionless coefficients, A_f and A_L are the sailing frontal and lateral area (respectively) of the emerged part of the vessel and V is the wind speed. The angle of incidence with respect to the fixed axis OX is given by $\beta_{V,OXYZ}$ and the angle relative to the vessel is given by β_V ($\beta_{V,OXYZ}=\beta_V+\psi$),, both defined in Figure 3. When the ship has her own speed, the angle of incidence β_V is corrected to consider the velocity of the hull.

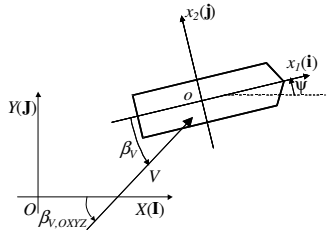

Figure 3 - Incident Wind Angles

The areas used for both vessels are given in Table 2. The dimensionless coefficients of forces and moment of wind on the hull and superstructure were calculated using the approach proposed by Isherwood (1973).

2.3 SHIP RESISTANCE

The resistance force is given by the expression:

$$F_X = \frac{1}{2}\rho S U^2 (C_f + C_r) \qquad (2)$$

where ρ is the density of water, U the speed in relation to the water, C_f is the resistance coefficient of friction and C_r the coefficient of shape and waves. The coefficient of friction is calculated by the ITTC approximation:

$$C_f \cong \frac{0{,}075}{(\log_{10} \mathrm{Re} - 2)^2} \qquad (3)$$

The coefficient C_r is calculated according to the statistics proposed based on regressions by Holtrop; Mennen (1982) and Holtrop (1984).

2.4 ADDITIONAL FORCES

In addition to the resistance, the transversal force and yaw moment due to the flow of water acting on the hull are also considered. The speed of water in the hull is denoted by Vc (Figure 5); α is the direction in relation to the hull and α_{OXYZ} is the direction in relation to the fixed reference ($\alpha_{OXYZ}=\alpha+\psi$).

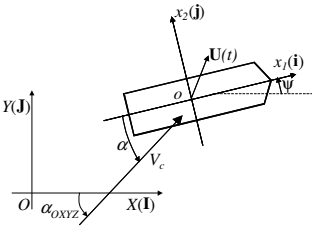

Figure 4 - Definitions to the Static Model of Current

The hydrodynamic forces are written as:

$$F_{1C} = \frac{1}{2}\rho V_{cr}^2 LT.C_x(\alpha); \quad F_{2C} = \frac{1}{2}\rho V_{cr}^2 LT.C_y(\alpha); \quad F_{6C} = \frac{1}{2}\rho V_{cr}^2 L^2 T.C_n(\alpha) \qquad (4)$$

where F_{1C} and F_{2C} are the forces in the longitudinal and transverse directions, respectively, F_{6C} is the yaw moment and C_x, C_y and C_n are the dimensionless coefficients of static current. These coefficients are calculated according to a heuristic short wing model presented in Leite et al. (1998),

and depend only on the main dimensions of the vessel. Terms that depends on the rotation of the hull (r) are evaluated from an extension of such model (Simos et al., 2001).

2.5 MAIN ENGINE

The estimated maximum power and thrust for the main propeller of the two vessels under study are presented in the table below:

Table 2 Characteristics of main thrusters

	Vessel A	Vessel B
Rated Power	25226 HP	15600 HP
Estimated Maximum Thrust	270 ton	167 ton

The calculation of force and torque acting on a propeller is based on the curves of the propeller, defined in terms of the dimensionless coefficient of progress J_0, given by:

$$J_0 = \frac{V_P}{n_P D_P} \tag{5}$$

where V_P is the speed of the propeller in the water (or the speed of the current projected into the propeller), n_P the rotation (in hertz) and D_P the diameter. The coefficients of thrust and torque K_Q and K_T are functions of the coefficient of forward J_0, and are defined by:

$$K_T = \frac{T_{Prop}}{\rho |n_P| n_P D_P^4}; K_Q = \frac{Q_{Prop}}{\rho |n_P| n_P D_P^5}; \eta = \frac{J_0 K_T}{2\pi K_Q} \tag{6}$$

where ρ is the density of water, T_{Prop} the thrust, Q_{Prop} the hydrodynamic torque of the propeller, and η the hydrodynamic efficiency in open water. Thus, considering a B-Screw propeller, the coefficients of thrust (K_T) and torque (K_Q) were obtained (Oosterveld, van Oossanen, 1975).

The effect of flow speed reduction into the propeller is modelled by the wake factor w. Thus, the speed Vp is given by (1-w) U, where U is the longitudinal speed of the vessel. For vessel A we considered w = 0.29, and for the vessel B is adopted the value w = 0.4. Also included is the reduction of the effect of thrust due to thruster-hull interference, modelled by the dimensionless factor t. Thus the real thrust is given by (1-t) T_{prop}, where the values adopted were of 0.18 (vessel A) and 0.19 (vessel B). The values were obtained by statistical regressions proposed in Holtrop; Mennen (1982) and Holtrop (1984).

A 2nd order dynamic system is implemented to represent the inertia of the propeller, resulting in a total reversal time of 300s.

2.6 BOW AND STERN THRUSTERS

The ships have tunnel thrusters at the bow and stern. Their main characteristics are presented in Table 4. The efficiency reduction of the thrusters due to the advance speed of the ship was also considered, according to data presented in Table 5.

Table 3 Characteristics of the bow and stern thrusters

	Vessel A	Vessel B
Power Bow	2416 HP	1971 HP
Thrust Bow	20 ton	20 ton
Power Stern	2146 HP	986 HP
Thrust Stern	20 ton	10 ton

Table 4 Loss of efficiency of propellers in tunnels

Velocity (knots)	Effectiveness (%)
1,3	100
3,0	75%
4,2	50%
5,5	25%
Above 6	0%

2.7 RUDDER

Vessel A has a conventional type rudder, with 10.1 m height and 5.75m chord, resulting in a total area of A_{rudder} = 58.1 m². The maximum turning angle is 35°.

Vessel B has a high lift Becker Rudder, with maximum angle of 65°, with 37m² approximate area. It was assumed, based on other ships, that the turning speed of the rudder for both vessels is limited to 2.8 °/ s.

Drag and lift forces are given by the dimensionless coefficients C_L and C_D:

$$F_D(\beta_{rudder}) = \frac{1}{2}\rho A_{rudder} C_D(\beta_{rudder}) V_{rudder}^2$$
$$F_L(\beta_{rudder}) = \frac{1}{2}\rho A_{rudder} C_L(\beta_{rudder}) V_{rudder}^2 \quad , \tag{7}$$

where F_D and F_L and the drag and lift forces respectively, C_D and C_L the dimensionless coefficients and V_{rudder} the relative velocity of the fluid onto the rudder (Figure 5).

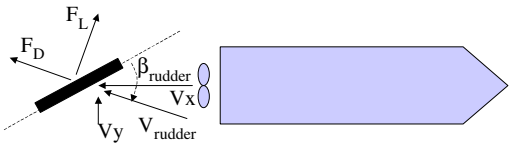

Figure 5 - Definitions for the modelling of the rudder

The speed of the propeller downstream flow V_x was calculated using an argument of conservation of momentum, resulting in:

$$V_x = \frac{1}{2}\left(V_i + \sqrt{V_i^2 + \frac{16}{\rho\pi D_P^2} T_{prop}}\right) \tag{8}$$

where V_i is the speed of the vessel. It results that the speed V_x is around 1.4 to 2 times the advance speed of the vessel, which is consistent with the curve presented in Lewis (1998). When the main propeller operates with reverse rotation, we adopt Vx = 0.

2.8 EFFECTS OF SHALLOW AND RESTRICTED WATER

The simulator includes the effects of restricted channels and

shallow water. In shallow water, the flow of water under the keel of the ship is accelerated, causing increased viscous forces and the consequent increase in frictional resistance of the vessel. Furthermore, the hull-generated wave length is modified, increasing the resistance due to wave generation. Additional masses, cross flow induced lateral forces and yaw moment are also increased because of the increased speed of flow. There are also effects on the propeller and rudder efficiency. Finally, it produces a sinking of the ship for high advance speeds (squatting).

These effects become significant when the relation between the depth of the channel (H) and the draft of the vessel (T) is smaller than 6. The models in the literature for shallow water are generally valid for H/T> 1.2. To take into account effects of very shallow water, where H / T <1.2 (in some cases, H / T <1, when the ship enters the mud bottom), hybrid models are employed. These combine the formulation for shallow water with models for navigation in muddy channels.

When navigating near the edge of channels, the speed of the flow between the channel and the ship's side is also increased, leading to a change in the field of pressure around the hull. Consequently, there is a lateral force of attraction toward the bank, while at the same time moment appears that tends to distance the bow from the bank.

2.9 SHALLOW WATER – RESISTANCE TO THE ADVANCE

Lewis (1998) presented a basic model for the effect of increased resistance in shallow water, considering also the width of the channel. We consider a ship in a channel of width b and depth H with maximum sectional area Ax and perimeter of submerged section p. The hydraulic radius R_H is defined as $R_H = (bH - A_x)/(b + 2H + p)$, so that in the case of unrestricted channel ($b \to \infty$) it is equivalent to the depth of the channel H. There is a change in the velocity of propagation of waves in a shallow and restricted channel in comparison with the case of open and unrestricted waters. In the latter case, the waves generated by the ship have speed $V_\infty^2 = gL_w / 2\pi$, where L_w is the wave length. Since the wave propagation speed depends on the depth, in a shallow channel the same wavelength will be generated with the ship speed given by $V_I^2 = gL_w / 2\pi \tanh(2\pi H / L_w)$. Thus, a relationship is obtain between the ship speeds in deep (V_∞) and shallow (V_i) water that result in the same resistance of waves:

$$\frac{V_i}{V_\infty} = \sqrt{\tanh\left(\frac{2\pi H}{L_w}\right)} = \sqrt{\tanh\left(\frac{gH}{V_\infty^2}\right)} \quad (9)$$

There is also an increase of frictional resistance, since the speed around the hull is greater due to restrictions imposed by the channel. Thus, the coefficient C_f, calculated for the ship speed V_i, corresponds to a smaller real speed V_h, since for the ship speed V_h , the flow speed around the hull is increased to V_i. The relationship between V_h and Vi is taken from Lewis (1998).

2.10 SHALLOW WATER – LATERAL FORCES AND ADDED MASSES

Ankudinov et al. (1990) presented the correction factor for the hydrodynamic derivatives Y_v, N_v, Y_r and N_r and the additional masses m_{22} and m_{66} according to the depth of the channel H, valid for H / T> 1.1 approximately. Using the results presented in Delefortrie et al. (2005), the curves were extrapolated to values up to H / T> 0.80. The derived Y_v and N_v are the slope of the curves of C_y and C_n for the incidence of 180°. Additionally, the values of Y_r and N_r appear explicitly in the short wing model, corresponding to forces dependent on the rotation of the hull. The correction of the added mass m_{11} was performed using the same correction factor of mass m_{22}. Note that the added mass of the ship (m_{22}) may increase up to 8 times compared to the value in deep water, which reflects the greater difficulty to manoeuvre the vessel in shallow waters.

For incidence angles higher than 40°, the hydrodynamic forces are primarily due to cross-flow. Thus, it was used the data from OCIMF (1994) for H / T> 1.1, and expanded to H / T <1 using data from Ankudinov et al. (1990).

2.11 SQUATTING

The dynamic sinking of the ship in shallow water is the phenomenon known as squatting. This effect reinforces the effect of shallow water, as it reduces the gap at the bottom of the hull. The formulation given by ICORELS (1980) is used here:

$$z_b(m) = 2.4\frac{\Delta}{Lpp^2}.\frac{Fr^2}{\sqrt{1-Fr^2}} \quad (10)$$

where z_b is the sinking of the hull and F_r the Froude number, given by $v/\sqrt{g.H}$.

2.12 RESTRICTED WATERS

We consider a ship with beam B sailing in a channel of width W at a distance y to the centre line of the channel. Lewis (1998) obtained the attraction forces Fy based on y and W, reproduced in Figure 12a, which uses the dimensionless factor $\overline{F}_Y = 0{,}5F_Y / \rho LTV^2$, where V the ship speed. The greater the proximity to the edge of the channel, or the smaller its width, the greater the force of attraction. There is also a correction for shallow water, which amplifies the effect of attraction toward the edge of the channel. Thus, the correction factor α is defined as $\alpha = F_Y(\mathrm{H/T}) / F_Y(\mathrm{H/T} = 1.4)$. The yaw moment M_z due to the proximity of the channel, which tends to move the bow away of the bank by defining the centre of application of the force as $\overline{x} = M_z / F_Y L$. The negative value indicates that the F_y force is applied at the aft part of the vessel.

3. CASE STUDIES

We shall report briefly on two real-world applications of this simulator.

3.1 PORT OF RIO GRANDE

The objective of this study was to investigate the impact of the presence of the oil platform P-53 upon the manoeuvres of ships in and out of the New Harbour of the Port of Rio Grande (RS/Brazil). The platform is a FPSO that is docked at a section of the harbour near its entrance for completion of its construction (see Figure 6a). According to the instructions of the Navy Port Authority, manoeuvres in and out of this harbour must be assisted by tugboats at bow and stern, without the use of the ship's thrusters. The simulator was prepared accordingly, with one tugboat of 32 ton of bollard pull at the bow and a tugboat of 50 ton of bollard pull at the stern (Figure 6b).

(a)

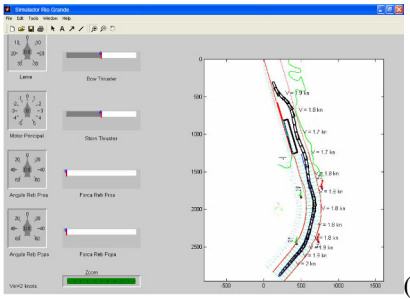
(b)

Figure 6 – (a) New Harbour at the Port of Rio Grande (b) Simulator's GUI

Several simulations were conducted considering different parameters: current speeds of 2 knots (ebb) and 1 knot (flow); South and East winds of 25 knots; ship entering bow first and stern first. Figure 7 illustrates one of the cases. We can see that the simulator allows the evaluation of the ship's trajectory, of her distance from the boundaries of the canal and from the P-53 platform, and of the forces and positions of the tugboats.

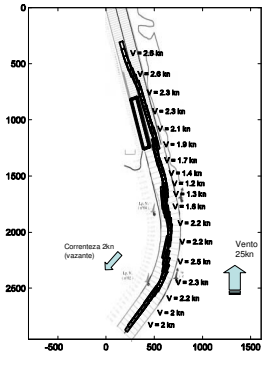

(a)

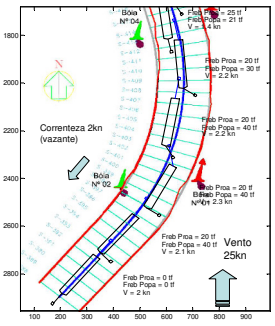

(b)

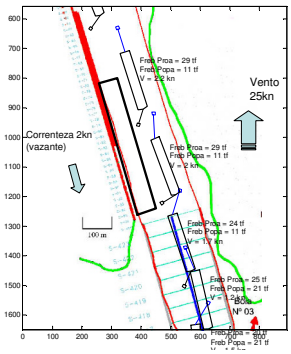

(c)

Figure 7 – Ebb current, South wind, stern first manoeuvre (a) Illustration of trajectory; (b) Detail of entrance curve; (c) Detail of passage by P-53

The study indicated that, regarding the presence of the P-53 platform and within the limits of the data employed (type of ships, environmental conditions, canal layout and bathymetry, tugboat configuration etc), the in and out manoeuvres at the New Harbour of the Port of Rio Grande are technically viable.

3.2 PORT OF ANTONINA

The purpose of this study was to use simulations to inspect the manoeuvring conditions along the canal (Figure 8b) and basin (Figure 8c) of the Ponta do Félix Terminal of the Port of Antonina (PR/Brazil). The canal has points of limited depth (Figure 8a), and it was of interest to evaluate the need for further dredging at some locations. In particular, the study tried to investigate the viability of operating with vessels larger than those served by the terminal up to that time.

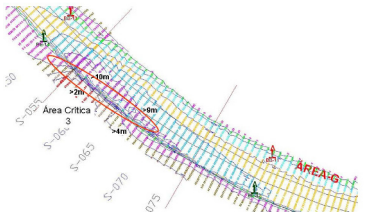

(a)

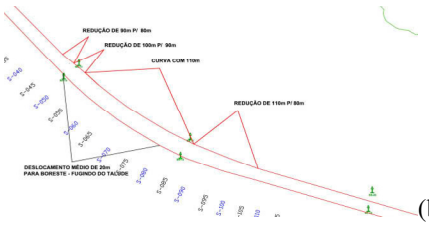
(b)

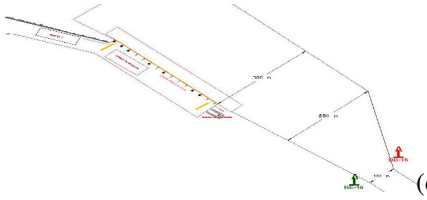
(c)

Figure 8 – Ponta do Félix Terminal (a) Curve with bank; (b) The canal; (c) The manoeuvring basin

Simulations were carried out representing the navigation along the canal, considering in and out manoeuvres, and two separate conditions of tide current. In every case the underkeel clearance was recorded, helping to determine the

need for additional dredging in some locations. Figure 9 shows an example of simulation. In the manoeuvring basin, berthing and unberthing manoeuvres were simulated, including the approximation and departure from the dock, and entrance and exit turns. For these manoeuvres there is the possibility of using the assistance of tugboats at bow and stern (up to 30 ton of bollard pull). Figure 10 depicts an example of an entrance manoeuvre with turn.

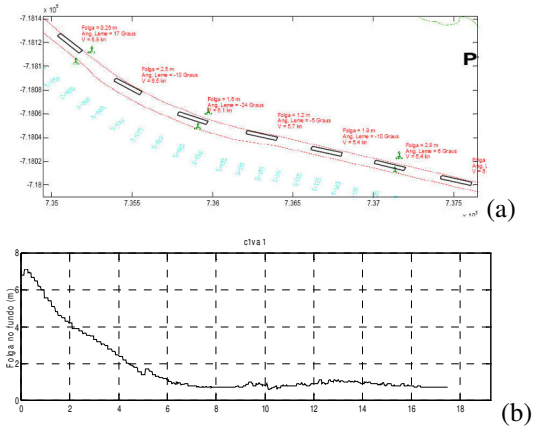

Figure 9 – (a) Simulated navigation along the canal; (b) Record of underkeel clearance

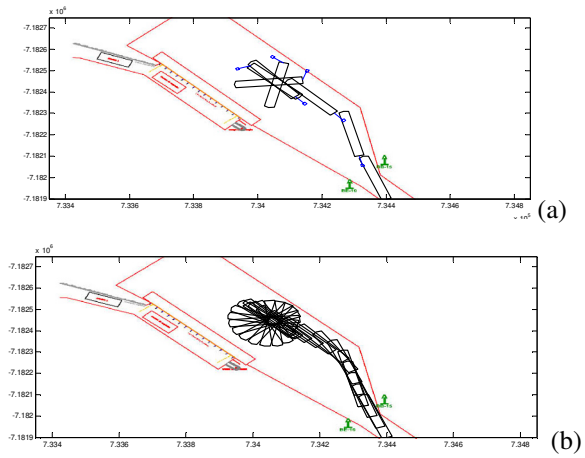

Figure 10 – (a) Simulation of entrance manoeuvre with turn showing position of tugboat; (b) Graphical record of ship trajectory

4. CONCLUSIONS

This paper described the development of a computer simulator to study ship manoeuvres in canals, basins, and other restricted water situations. The simulator incorporates mathematical models to represent environmental agents, control elements, and the effect of shallow and restricted waters. It can be easily customized with the data for any specific port or terminal, and two real-world cases of application of this simulator were described. The system implements an interactive graphical interface through which the user has control over the same basic variables at the disposal of a real pilot (rudder angle, engine speed, azimuth and other thrusters, and tugboats).

ACKNOWLEDGMENTS

The authors would like to thank QUIP S/A and TPPF S/A for their permission to publish results of the technical studies they sponsored. J. R. de Souza Junior and E. A. Tannuri are partially supported by CNPq through Research Grants 307417/2006-9 and 301686/2007-6, respectively.

REFERENCES

ANKUDINOV, V.K., MILLER, E.R., JAKOBSEN, B.K., DAGGETT, L.L., Manoeuvring performance of tug/barge assemblies in restricted waterways**, Proceedings MARSIM & ICMS 90**, Japan, pp. 515-525, 1990.

DELEFORTRIE, G., ET AL., Modelling navigation in muddy areas through captive model tests, **J. Mar Sci Technol**, 10:188-202, 2005.

HOLTROP, J. *A Statistical Reanalysis of Resistance and Propulsion Data,* **International Shipbuilding Progress**, Vol. 31, 1984.

HOLTROP, J.; MENNEN, G.G.J. *An Approximate Power Prediction Method*, **International Shipbuilding Progress**, Vol. 89, 1982.

ICORELS (International Comission for the Reception of Large Ships), Report of Working Group IV, **PIANC Bulletin**, No. 35, Supplement, 1980.

ISHERWOOD, R.M. *Wind resistance of merchant ships*, **Proceedings of Royal Institution of Naval Architects**, 1973.

LEITE, A.J.P. et al. Current forces in tankers and bifurcation of equilibrium of turret systems: hydrodynamic model and experiments, **Applied Ocean Research**, No.20, pp.145-56, 1998.

LEWIS, E.V. **Principles of Naval Architecture**, The Society of Naval, Jersey City, 1998.

OCIMF, Oil Companies International Marine Forum, Prediction of wind and current loads on VLCCs, Technical Report, 1982.

OOSTERVELD M.W.C. ; VAN OOSSANEN P. *Further Computer-Analyzed Data of Wageningen B-Screw Series*, I.S.P., Vol. 22, No. 251, July 1975.

SIMOS, A.N. et al. A quasi-explicit hydrodynamic model for the dynamic analysis of a moored FPSO under current action, **Journal of Ship Research**, Vol.45, No.4, pp289-301, 2001.